

3. V. V. Blazhenkov, A. V. Bukharov, and A. A. Vasil'ev, Physical Problems in the Study of Monodispersed Systems [in Russian], No. 147, Moscow (1987).
4. V. I. Bezrukov, V. D. Spiridonov, and Yu. V. Syshchikov, XV All-Union Conference "Practical Questions in the Physics of Aerodispersed Systems" [in Russian], Vol. 1, Odessa (1989), p. 47.
5. V. I. Bezrukov and V. D. Spiridonov, Electrodroplet-Jet Technology in the Realization of the "Intensifikatsiya-90" Program [in Russian], Leningrad (1989), pp. 9-17.
6. V. I. Bezrukov (ed.), Flexible Automatic Electrodroplet-Jet Systems for Part Marking in Ship Construction [in Russian], Leningrad (1988).

INDUCTIONAL CHARGING OF MONODISPERSED DROPS FORMED IN THE INDUCED
CAPILLARY BREAKDOWN OF LIQUID JETS

V. V. Blazhenkov, A. V. Bukharov,
A. A. Vasil'ev, and S. N. Panasov

UDC 621.319.7.001:517.958

Theoretical and experimental data on the inductional charging of monodispersed liquid drops formed in the induced capillary breakdown of liquid jets are given.

The preparation of fluxes of monodispersed drops with dosed electric charges which may be controlled by means of electric and magnetic fields is one of the basic elements of electrodrop-jet [1] and cryodisperse [2] technology.

The method of inductional charging of monodispersed drops of conducting liquids formed as a result of the induced capillary breakdown of liquid jets (ICBJ) is investigated in the present work. The results of analytical and numerical calculations are given, as well as experimental data on the charges induced at the drops in electric fields of various configurations. The experimental and theoretical data are compared.

In inductional charging, the potential applied between the electrodes (the charging electrode most often takes the form of a plane with a hole, a ring, or a cylinder; the second electrode is an attachment to the ICBJ generator and the intact part of the jet itself) induces some charge distribution along the jet; this distribution depends on the concentration and mobility of the charge carriers in the liquid volume and also on the time of drop formation in ICBJ.

The charge induced at the drop may be expressed in terms of the its equivalent capacitance and the potential at the charging electrode V : $Q = -C\alpha V$; here α takes account of the correction for the local value of the potential at the point of breakdown.

The capacitance of the drop is determined by its size and shape. For a spherical drop, the capacitance is $C = 4\pi\epsilon\epsilon_0 R_d$. It must be taken into account that the shape of the surface of the intact part of the jet and the charges at all the previously formed drops in the flux influence the magnitude of the charge.

The influence of the shape of the drop may be estimated from the change in capacitance of an ellipsoid of revolution as a function of its eccentricity, since the drops take this form at the instant of breakaway from the jet in ICBJ. Data on the charges at the drops as a function of the eccentricity obtained by experiment (points) and calculation (continuous curve) are shown in Fig. 1.

Because of the finite electrical conductivity of the liquid, the inductional charging of the drop does not occur instantaneously. To describe the dynamics of the charging process, it is expedient to represent the charged section of the jet and the charging device as a series RC circuit in which the resistance R is determined by the electrical conductivity of the liquid being dispersed ρ , the diameter D_j , and the length of the intact part of the jet L_j :

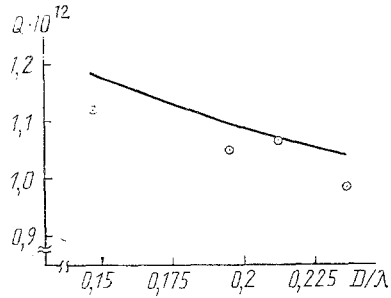


Fig. 1

Fig. 1. Dependence of the charge at the drop Q, C , on its eccentricity: points) experiment; curve) theoretical results.

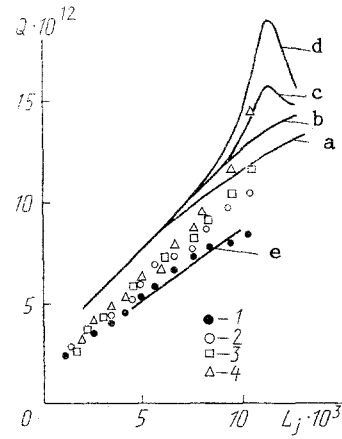


Fig. 2

Fig. 2. Dependence of the charge at the drop Q, C , on the length of the intact section of the drop, m , in charging in the field of a plane capacitor with an aperture; the distance between the capacitor plates $L_0 = 11.6 \cdot 10^{-3}$ m; potential difference $V = 900$ V; aperture diameter of attachment $D_N = 2 \cdot 10^{-4}$ m, $\alpha = 0.7$; experimental data: 1) $D_p = 10^{-2}$ m; 2) $5 \cdot 10^{-3}$; 3) $3 \cdot 10^{-3}$; 4) $2 \cdot 10^{-3}$ m; results of numerical calculation: a) $D_p = 10^{-2}$ m; b) $5 \cdot 10^{-3}$; c) $3 \cdot 10^{-3}$; d) $2 \cdot 10^{-3}$ m; e) results of analytical calculations.

$$R \approx \rho \frac{4L_j}{\pi D_j^2}.$$

An expression relating the charging parameters may be written for the series RC circuit

$$\alpha V = jR + \frac{1}{C} \int j dt,$$

and the charge at the drop Q is

$$Q = \int j dt.$$

The solution of this equation gives the transition characteristic of the system with instantaneous establishment of the potential V at the charging electrode

$$Q(t) = \alpha VC (1 - \exp(-t/RC)).$$

This solution corresponds to an integrating aperiodic element with a time constant of RC . For effective charging, the residence time of the drop close to the charging electrode must be greater than the time of the transient process; for ICBJ, this means that $RC \ll 1/f$ or $\rho \ll \pi L_j^2 / (f L_j R_d)$. In these conditions, the liquid jet may be regarded as an ideal conductor.

For typical parameters of devices in electrodrop-jet technology ($D_j \approx R_d = 10^{-4}$ m; $L_j = 10^{-3}$ m; $f \approx 10^4$ - 10^5 Hz), a lower bound is obtained for the electrical conductivity of the liquid being dispersed in inductive charging: $\rho \ll 3 \cdot 10^4 \Omega \cdot m$.

The electric charge induced at the drops is calculated by numerical and analytical methods.

1. Analytical calculations of the charges induced at monodispersed drops are based on the model of [4], with the following simplifications: the surface of the intact part of the jet is assumed to be cylindrical; the symmetry axes of the jet, the drop flux, and charging electrodes coincide; the parameters of the drop flux and the charging electrodes coincide; the parameters of the drop flux and the charging potential do not vary over time; no account is taken of distortion of the electric field close to the aperture and the edge of the charging electrode.

In this case, the density of the charges induced in the jet q is a function only of one coordinate z and, according to the superposition principle, is composed of the charge density $q_e(z)$ induced by the charging electrode and the charge density $q_d(z)$ induced in the jet by the previously charged drops of the flux of length L_d

$$q(z) = q_e(z) + q_d(z). \quad (1)$$

Within the framework of this model the charge Q acquired by the drop on separation from the jet is determined by the charge induced at the cylindrical section of the jet of length $\lambda = V_j/f$, equal to the excitation wavelength of the induced capillary ICBJ (i.e., in the part of the jet from which the next drop is formed)

$$Q = \int_{L_j - \lambda}^{L_j} q(z) dz. \quad (2)$$

Substituting Eq. (1) into Eq. (2), an expression for the charge is obtained

$$Q = \int_{L_j - \lambda}^{L_j} q_e(z) dz + \int_{L_j - \lambda}^{L_j} q_d(z) dz.$$

To find q_e and q_d , the axisymmetric potential $\varphi(r, z)$ created by the charging electrode and the flux of macroparticles is expressed in the form

$$\varphi(r, z) = \sum_{m=0}^{\infty} \frac{(-1)^m}{(ml)^2} \varphi^{(2m)}(z) \left(\frac{r}{2}\right)^{2m} = \varphi(z) - \frac{r^2}{4} \varphi''(z) + \dots$$

Close to the surface of the thin ($R_j \ll L_j$) jet, only the first term need be retained in this expression, i.e., the dependence of the charge-inducing potential on the radial coordinate may be neglected. From the equipotential condition of the thin conducting cylindrical rod in the external field $\varphi_d(z)$, the following equation for $q_d(r)$ is obtained

$$q_d(z) \ln \frac{4(L_j - z)z}{R_j^2} + \int_0^{L_j} \frac{q_d(z') - q_d(z)}{|z' - z|} dz' = -\varphi_d(z). \quad (3)$$

This equation is solved by an iterative method [4], permitting the determination of the correction to the drop charge due to the influence of the macroparticle flux

$$Q = \frac{\int_{L_j - \lambda}^{L_j} q_e(z) dz}{1 + 0,3(c_0 + \ln L_d/\lambda)/\ln(2L_j/R_j)}, \quad L_d/\lambda \geq 2. \quad (4)$$

As is evident from Eq. (4), the action of the first few drops decreases the charge at the drop Q by an amount of the order of 10%; for longer chains of macroparticles $L_d \sim 2L_j$, the decrease in Q may amount to several tens of percent. To determine q_e in the field of a plane capacitor, neglecting distortion of the charging field due to the apertures in the plates, an equation analogous to Eq. (3) is used

$$q_e(z) \ln \frac{4(L_j - z)z}{R_j^2} + \int_0^{L_j} \frac{q_e(z') - q_e(z)}{|z' - z|} dz' = \frac{V}{D} z,$$

where V is the potential difference between the plates, which leads to an expression for $q_e(z)$

$$q_e(z) = (Vz/2D) (\ln(2z/R_j) - 1),$$

and substitution of this expression into Eq. (4) gives the value of Q in the field of plane electrodes

$$Q_c = \frac{2\pi\epsilon_0\lambda L_j V}{D (\ln(2L_j/R_j) - 1) [1 + 0,3(c_0 + \ln(L_d/\lambda))/\ln(2L_j/R_j)]}$$

Analytical expressions for the charge at a drop induced by annular and cylindrical charging electrodes may be obtained by an analogous method

$$Q_r = \{2\pi\epsilon_0\lambda V\} \left\{ \sqrt{1 + \left(\frac{L_j - D}{R_r}\right)^2} \left(\ln 2 \frac{L_j}{R_j} - 1\right) \ln\left(8 \frac{R_r}{r_r}\right) \left[1 + 0,3 \left(c_0 + \ln \frac{L_d}{\lambda}\right) / \ln \frac{2L_j}{R_j}\right] \right\}^{-1},$$

$$Q_i = \frac{4\pi\epsilon_0\lambda V}{[2 \ln(R_t/R_j) + \ln(1 + R_t/4L_j^2)] [1 + 0,3(C_0 + \ln L_d/\lambda)/\ln(2L_d/L_j)]},$$

where R_r , r_t , and R_t are the dimensions of the ring and the cylinder.

2. In the numerical calculation, the charge is found using a Laplacian equation in a cylindrical coordinate system

$$\frac{1}{r} \frac{\partial}{\partial r} \left(r \frac{\partial \varphi}{\partial r} \right) + \frac{\partial^2 \varphi}{\partial z^2} = 0.$$

This equation is approximated by a five-point conservative scheme on a grid that is nonuniform (since there is a difference of one or two orders of magnitude between the jet and electrode diameters) over the radius

$$(\varphi_{ij+1} - \varphi_{ij}) q_N + (\varphi_{ij-1} - \varphi_{ij}) q_S + (\varphi_{i-1j} - \varphi_{ij}) q_W + (\varphi_{i+1j} - \varphi_{ij}) q_e = 0,$$

where

$$q_N = (r_j + dr_j) \frac{2dz}{dr_{j+1} + dr_j},$$

$$q_S = (r_j - dr_j) \frac{2dz}{dr_j + dr_{j-1}},$$

$$q_e = r_j \frac{dr_j}{dz}, \quad q_W = r_j \frac{dr_j}{dz},$$

r_j , dr_j , dz characterize the dimensions and position of the elementary cell.

Each subsequent elementary cell is 9-10% larger in radial dimension than its predecessor, on moving away from the axis of the system.

In accordance with the above assumptions, the equations are solved with the following boundary conditions

$$\varphi = V|_{z, r \in S_i} \quad (S_i \text{ is the surface of the charging electrode});$$

$$\varphi = 0|_{z=0} \quad (\text{the plane of the ICBJ-generator attachment});$$

$$\varphi = 0|_{r=R_j; z=L_j} \quad (\text{at the jet surface}).$$

To simplify the numerical calculations, the region of integration is bounded by the maximum values R_{\max} and z_{\max} , which are chosen so that variation in these values by a factor of 1.5 changes the results of the calculations by no more than 5%. At these boundaries, the boundary condition is zero normal component of the field (i.e., no charges beyond its limits)

$$\frac{\partial \varphi}{\partial z} = 0 \quad \text{or} \quad \frac{\partial \varphi}{\partial r} = 0.$$

Numerical calculation is realized by successive approximation using the upper-relaxation method, which ensures a stronger interdependence of neighboring cells and therefore a higher rate of convergence

$$\varphi_{ij}^+ = (1 - R_{rel})\varphi_{ij} + R_{rel} (q_W\varphi_{i-1j} + q_N\varphi_{ij+1} + q_e\varphi_{i+1j} + q_S\varphi_{ij-1})/q_{\text{sum}},$$

$$q_{\text{sum}} = q_N + q_W + q_e + q_S.$$

The characteristics of inductional charging of monodisperse drops are studied experimentally by means of an automated unit based on a MERA-60 computer and interface modules in the CAMAC standard. The apparatus permits the maintenance of time-stable ICBJ parameters (liquid flow rate, length of the intact part of the jet, size and velocity of the monodispersed particles) with high accuracy by means of a digital negative-feedback system. This is important since, as is evident from the theoretical and experimental results, small changes in length of the intact part of the jet or the drop size many significantly influence the magnitude of the induced charges.

As well as specification and stabilization of the ICBJ parameters, the automated experimental unit ensures the application of program-controlled potentials to the charging electrodes and also facilitates diagnostics of the geometric (size, velocity, and dispersion) and electrical (integral and individual charge at the drops and their dispersion) characteristics.

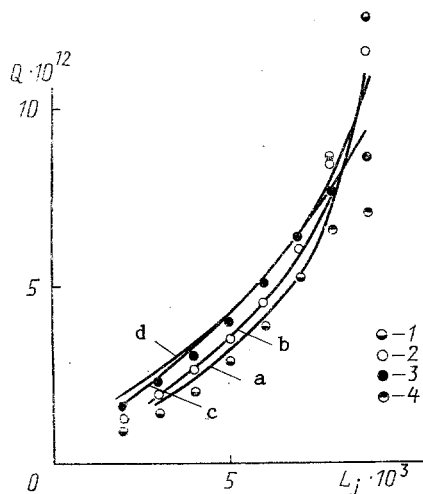


Fig. 3

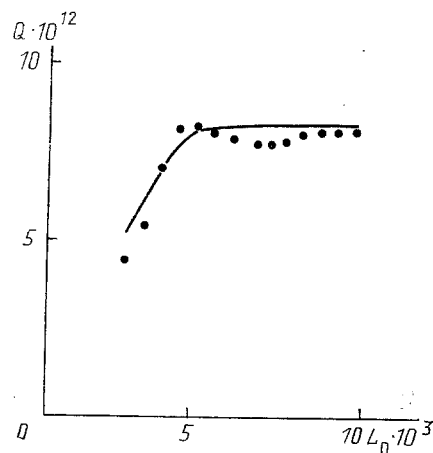


Fig. 4

Fig. 3. Dependence of the charge at the drop Q , C, on the length of the intact part of the jet, m , on charging in the field of a ring at a distance of $10.4 \cdot 10^{-3}$ m from the attachment output; charging potential $V = 900$ V; $D_N = 2 \cdot 10^{-4}$ m; $\kappa = 0.7$; experimental data: 1) $D_C = 2 \cdot 10^{-3}$ m; 2) $3 \cdot 10^{-3}$; 3) $5 \cdot 10^{-3}$; 4) $8 \cdot 10^{-3}$ m; the results of the numerical calculations: a) $2 \cdot 10^{-3}$ m; b) $3 \cdot 10^{-3}$; c) $5 \cdot 10^{-3}$; d) $8 \cdot 10^{-3}$ m.

Fig. 4. Dependence of the charge at the drop Q , C, on the position of the charging electrode relative to the attachment of the ICBJ generator, m ($z = 0$), on charging in the field of a cylindrical capacitor; charging potential $V = 500$ V; aperture diameter of attachment $D_N = 2 \cdot 10^{-4}$ m; $\kappa = 0.7$; cylinder length $H_C = 6 \cdot 10^{-3}$, diameter $D_C = 2 \cdot 10^{-3}$ m; points) experiment; curve) numerical calculation.

Variation in length of the intact part of the jet and in shape of the monodisperse drops is accomplished by controlling the amplitude of excitation without changing the wave number of breakdown ($\kappa = 0.69$).

The shape of the charged drops is recorded by means of a TV camera, the integral charge by means of a Faraday cylinder, and the charges of individual drops by means of a probe. All the signals recorded are converted to digital code by means of CAMAC analog-digital converters and fed to the microcomputer for analysis. The data obtained are shown in Figs. 2-4.

As is evident, the theoretical values adequately described the qualitative behavior and numerical values of the experimental data. The overestimation (10-30%) of the charge at the drops obtained by the numerical method is explained in that these calculations take no account of the influence of the charges of the flux drops.

On all the curves, the dependence of the charge at the drop on the position of the point of jet breakdown with respect to the charging electrode may be divided into two characteristic regions. The first corresponds to the case where the drops breaking away from the jet are close (of the order of 10 jet radii) to the charging electrode. In this region, significant increase in the charge of the drop is seen as the point of drop formation approaches the charging electrode with constant charging potential V . The second region corresponds to the case where the point of drop formation is at a significant distance from the charging electrode (or its edge for a cylinder). In this case, the charge induced at the drop is proportional to the local (at the point of drop breakaway from the jet) potential in the electrode system, when the liquid jet itself is absent. If the electrode is a plate with an aperture, the change in the charge is practically linear in space; in the case of a ring, it varies analogously to the change in potential of a charged ring above a plane; for a cylinder, the change is analogous to the potential change along the cylinder axis.

From the viewpoint of constructing devices in electrodrop-jet technology, a cylindrical charging electrode is more promising, with less rigorous requirements on the stability of the length of the intact part of the jet.

NOTATION

Q , charge induced at the drop; C , equivalent capacitance; V , potential at the charging electrode; R_d , radius of charged drop; R , resistance; ρ , electrical resistivity of dispersing liquid; D_j , L_j , diameter and length of intact part of jet; D_p , diameter of aperture in plate; D_c , ring diameter; D_N , aperture diameter of attachment; q , charge density induced at jet; L_d , length of flux; $C_0 = 0.577$, Euler constant; D , distance between plates; r_j , dr_j , dz characterize the dimensions and position of the elementary cell; S_i , surface of charging electrode; φ_{ij}^+ , φ_{ij} , two successive approximations; R_{el} , upper-relaxation coefficient chosen empirically in the range 1.90-1.95; R_r , r_r , R_t , dimensions of ring and cylinder.

LITERATURE CITED

1. V. S. Nagorny, *Electrodrop-Jet Recording Devices* [in Russian], Leningrad (1988).
2. V. A. Grigor'ev, *Vestn. Akad. Nauk SSSR*, No. 4, 84-90 (1987).
3. L. D. Landau and E. M. Lifshits, *Continuum Electrodynamics* [in Russian], Moscow (1957).
4. V. V. Blazhenkov, A. V. Bukharov, and A. A. Vasil'ev, in: *Collection of Scientific Works* [in Russian], No. 149, Moscow Power Institute, Moscow (1987), pp. 37-46.
5. A. V. Bukharov and A. S. Sidorov, in: *Collection of Scientific Works* [in Russian], No. 185, Moscow Power Institute, Moscow (1988), pp. 58-63.
6. A. V. Bukharov and S. I. Shcheglov, in: *Collection of Scientific Works* [in Russian], No. 119, Moscow Power Institute, Moscow (1986), pp. 91-98.

PATH OF DROP JET AND SINGLE DROP IN ELECTRODROP-JET DEVICES

V. I. Bezrukov, A. A. Vydrik,
and E. F. Sukhodolov

UDC 532.51:681.327

A mathematical model describing the path of a drop jet and a single drop in all practically important deflecting systems of electrodrop-jet devices is described.

The deflection and path control of drops of working liquid are the most important processes of electrodrop-jet technology. However, there are very few engineering solutions for deflecting drop systems (DS), with practically no choice, and very precise analysis is required for the existing DS in order to ensure optimal operating conditions of the electrodrop-jet device.

The desirable complete analogy with ion-electron DS is not very useful here, since for macroparticles (drops) there arise phenomena which are not seen for electrons and ions and which significantly change the particle behavior in DS [1, 2]. In particular, because of the small ratio of the transverse dimension of the deflecting-field region and the macrodiameter, inhomogeneity of the field and edge effects play an important role where they may be disregarded in electron DS; because of the relatively small drop velocity due to the jet velocity, "cutoff" of the field is not possible here, in contrast to ion-electron DS [3]. Because $r_d \gg r_e$, aerodynamic effects that are not characteristic of ordinary DS begin to appear, leading to new phenomena such as change in the drop acceleration, coalescence of the drops into double and triple conglomerates, etc. Therefore, the standard (for electron DS) use of series expansion in terms of the distance from the drop-flux axis in calculating the error of drop positioning is inexpedient in modeling the path in drop DS. A more informative and physically correct approach is trajectory analysis on a computer, including the solution of the field problem, integration of the equations of drop motion, and determining and optimizing the DS characteristics.

In the present work, on the basis of such analysis, a model of drop-flux motion in DS with electrodes in the form of solids of revolution, the generatrix of which L is a segment of a straight line or a second-order curve arbitrarily oriented relative to the direction of

Elektrokaplestruinaya Tekhnologiya Engineering Center, Leningrad Institute of Precision Mechanics and Optics. Translated from *Inzhenerno-fizicheskii Zhurnal*, Vol. 60, No. 4, pp. 652-655, April, 1991. Original article submitted July 31, 1990.